Departamento de Genética e Biologia Evolutiva - IB/BIO   Artigos e Materiais de Revistas Científicas - IB/BIO

2014-10

Phylogeny and historical biogeography of gnateaters (Passeriformes, Conopophagidae) in the South America forests

Phylogeny and historical biogeography of gnateaters (Passeriformes, Conopophagidae) in the South America forests

Henrique Batalha-Filho [a,b,*], Rodrigo O. Pessoa [c], Pierre-Henri Fabre [d,e], Jon Fjeldså [d], Martin Irestedt [f], Per G.P. Ericson [f], Luís F. Silveira [g], Cristina Y. Miyaki [a]

[a] Departamento de Genética e Biologia Evolutiva, Instituto de Biociências, Universidade de São Paulo, São Paulo, SP, Brazil
[b] Departamento de Zoologia, Instituto de Biologia, Universidade Federal da Bahia, Salvador, BA, Brazil
[c] Centro de Ciências Biológicas e da Saúde, Universidade Estadual de Montes Claros, Montes Claros, MG, Brazil
[d] Center for Macroecology, Evolution and Climate at the Natural History Museum of Denmark, University of Copenhagen, Copenhagen, Denmark
[e] Harvard Museum of Comparative Zoology, 26 Oxford Street, Cambridge, MA 02138, USA
[f] Department of Bioinformatics and Genetics, Swedish Museum of Natural History, Box 50007, SE-104 05 Stockholm, Sweden
[g] Museu de Zoologia, Universidade de São Paulo, São Paulo, SP, Brazil

ARTICLE INFO

ABSTRACT

We inferred the phylogenetic relationships, divergence time and biogeography of Conopophagidae (gnateaters) based on sequence data of mitochondrial genes (*ND2*, *ND3* and *cytb*) and nuclear introns (*TGFB2* and *G3PDH*) from 45 tissue samples (43 *Conopophaga* and 2 *Pittasoma*) representing all currently recognized species of the family and the majority of subspecies. Phylogenetic relationships were estimated by maximum likelihood and Bayesian inference. Divergence time estimates were obtained based on a Bayesian relaxed clock model. These chronograms were used to calculate diversification rates and reconstruct ancestral areas of the genus *Conopophaga*. The phylogenetic analyses support the reciprocal monophyly of the two genera, *Conopophaga* and *Pittasoma*. All species were monophyletic with the exception of *C. lineata*, as *C. lineata cearae* did not cluster with the other two *C. lineata* subspecies. Divergence time estimates for Conopophagidae suggested that diversification took place during the Neogene, and that the diversification rate within *Conopophaga* clade was highest in the late Miocene, followed by a slower diversification rate, suggesting a diversity-dependent pattern. Our analyses of the diversification of family Conopophagidae provided a scenario for evolution in *Terra Firme* forest across tropical South America. The spatio-temporal pattern suggests that *Conopophaga* originated in the Brazilian Shield and that a complex sequence of events possibly related to the Andean uplift and infilling of former sedimentation basins and erosion cycles shaped the current distribution and diversity of this genus.

© 2014 Elsevier Inc. All rights reserved.

1. Introduction

The origin of the South American rain forest biota has fascinated naturalists since Wallace's days (Wallace, 1852), and several hypotheses have been evoked to explain the history of diversification (review in Moritz et al., 2000) in this highly biodiverse region (Myers et al., 2000). For many years the Pleistocene refuge hypothesis (Haffer, 1969; Vanzolini and Williams, 1970) was assumed to represent the principal mechanism to explain diversification in the Amazon basin and other lowland rainforest regions in South America (Carnaval and Moritz, 2008; Whitmore and Prance, 1987). However, not all paleoecological data supported the presence of the postulated non-forested barriers during the Pleistocene (Bush and de Oliveira, 2006; Colinvaux et al., 2000), and phylogenetic analyses indicated that most diversification events in this region predate the Pleistocene climatic oscillations (Hoorn et al., 2010).

In the recent years, new aspects of land surface evolution have been evoked to explain biogeographic patterns in the Amazon area, such as changes in drainage patterns and sedimentation within the large wetlands that existed in western Amazon during the Miocene (Wesselingh et al., 2002), and the role of Andean uplift on drainage patterns of its lowlands (Antonelli and Sanmartín, 2011; Hoorn et al., 2010; Hoorn et al., 2013). The uplift of the Andes also triggered a climate change across the continent (Insel et al., 2009), as this mountain belt formed a barrier that retained moisture from the Atlantic Ocean. Thus, these events that occurred before the Pleistocene seem to have been important for the evolution of Neotropical biota (Antonelli et al., 2009; Lohmann et al., 2013;

Weir and Price, 2011). However, lineage diversification events seem to have occurred during all the Tertiary and Quaternary, even including the Pleistocene (Rull, 2008, 2011a, 2011b).

The hypothesis by Wallace (1852) that rivers could be barriers to dispersal and that this could lead to speciation, received new attention as geological evidence suggested a recent (Plio-Pleistocene) establishment of the Amazonian drainage channel to the Atlantic Ocean (Campbell et al., 2006; Latrubesse et al., 2010). This scenario has been shown to be congruent with recent divergence of avian populations across the river (Fernandes et al., 2012; Maldonado-Coelho et al., 2013; Ribas et al., 2012). According to this scenario, the Purus Arch (at 62°W) formed an eastern limit bounding the Solimões wetland system in western Amazonia until 9.5–6 Myr (Latrubesse et al., 2010), when the Amazon River broke through this barrier to drain toward the Atlantic Ocean.

To further investigate these historical scenarios, the gnateaters (Passeriformes: Conopophagidae) can be a good study case. These birds are an old lineage of New World suboscines (~41 Ma; Ohlson et al., 2013) that, in turn, evolved within South America, with only a few subclades colonizing Central and North America as part of the great American interchange (Smith and Klicka, 2010; Weir et al., 2009). The gnateaters presumably form a monophyletic family (Ohlson et al., 2013). They are endemic to the Neotropical region and associated with mesic *Terra Firme* forest. Therefore, they were likely limited by the distribution of flat and hydrologically unstable depositional landscapes of the Amazonian floodplains. The family was long defined to comprise only the genus *Conopophaga* (Whitney, 2003), but recent molecular phylogenies have placed *Pittasoma* (formerly Formicariidae) as sister to this genus (Moyle et al., 2009; Ohlson et al., 2013; Rice, 2005). Thus, Conopophagidae currently comprises two genera and ten species (Remsen et al., 2013) that live in the understorey of humid forests (Ridgely and Tudor, 1994). The genus *Pittasoma* has two species (*P. michleri* and *P. rufopileatum*) distributed in Central America and northwestern South America (Chocó region). The genus *Conopophaga* includes eight species (*C. lineata*, *C. aurita*, *C. roberti*, *C. peruviana*, *C. ardesiaca*, *C. castaneiceps*, *C. melanops*, and *C. melanogaster*), most polytypic and all endemic to South America (Fig. 1). Given the distributions of gnateater species through most of South America's tropical forests (Whitney, 2003), and the relative old age of the clade (Ohlson et al., 2013), we expect that the evolutionary history of this group should reflect the major events of landscape history in these regions. Thus, a reconstruction of the phylogenetic history of gnateaters would provide a useful framework to further test the origin of extant Neotropical biodiversity, as they evolved in "splendid isolation" within South America during the Tertiary (Ricklefs, 2002).

In this study, we infer the phylogenetic relationships, divergence time and biogeography of Conopophagidae by using mitochondrial and nuclear genes of a comprehensive taxon sampling of the family. In addition, we examine the diversification within *Conopophaga* by using a wide geographic sampling, and analyze its diversification rates through time, as well as its ancestral distribution. To shed light on the gnateaters' evolution we want to answer two main questions: (i) what are the phylogenetic relationships among species and subspecies of *Conopophaga*, and how these relationships correspond to currently defined species limits? and (ii) can the tempo and sequence of speciation events be associated with described events in the landscape history of South America?

2. Materials and methods

2.1. Taxon sampling and molecular methods

In order to recover the phylogenetic relationships within Conopophagidae, we analyzed 45 samples (43 *Conopophaga* and 2 *Pittasoma*) from the ingroup (Fig. 1; Table S1 in supplementary material), representing all currently recognized species of the family. For most species we included at least two individuals and for polytypic species most subspecies were sampled. In total we included 14 of the 18 recognized subspecies of genus *Conopophaga* (Whitney, 2003). *Melanopareia maranonica* was used as outgroup following Moyle et al. (2009).

DNA was extracted from tissues (muscle or blood) following Bruford et al. (1992). For most samples, we sequenced three mitochondrial genes – cytochrome b (*cytb*), NADH dehydrogenase subunit 2 (*ND2*) and NADH dehydrogenase subunit 3 (*ND3*); and two nuclear introns – glyceraldehyde-3-phosphodehydrogenase intron 11 (*G3PDH*) and transforming growth factor beta 2 intron 5 (*TGFB2*). Primers used to amplify these genes are given in Table S2 in supplementary material. PCR (25 μL) contained template DNA (50 ng), 1X of *Taq* buffer (GE Healthcare), dNTPs (0.32 μM), 0.5 μM of each primer and 0.5 U of *Taq* polymerase (GE Healthcare). PCR conditions were as follows: an initial denaturation step at 94 °C for 3 min and 30 s; followed by 35 or 40 cycles at 94 °C for 35 s, annealing temperature for 40 s and 72 °C for 1 min; plus a final extension step at 72 °C for 9 min. Annealing temperatures were as follows: *cytb*, *ND3*, and *ND2*-56 °C; *G3PDH*-63 °C; and *TGFB2*-60 °C.

Amplicons were purified using polyethylene glycol 20% (PEG) precipitation (Sambrook et al., 1989) or a mixture of Exonuclease 1/FastAP (Thermo Scientific). DNA was directly sequenced in both directions with the same amplification primers using Big Dye terminator 3.0 cycle sequencing kit (Applied Biosystems) following the manufacturer's protocol. Sequences were analyzed in an automated sequencer ABI PRISM 3100 (Applied Biosystems). Some samples were sequenced at the Macrogen sequencing service (Macrogen Inc., Seoul, South Korea).

Electropherograms were inspected and assembled in contigs using CodonCode Aligner v. 3.7 (CodonCode Inc.). Heterozygous sites in nuclear introns were coded according to IUPAC code when double peaks were present in both strands of the same individual's electropherograms. Sequences were aligned using the CLUSTAL W method (Higgins et al., 1994) in MEGA5 (Tamura et al., 2011). All alignments were inspected and corrected visually.

2.2. Phylogenetic analyses

We used Bayesian inference (BI) and maximum likelihood (ML) to estimate the phylogeny of Conopophagidae based on a concatenated sequence matrix of five partitions (*ND3*, *ND2*, *cytb*, *G3PDH*, and *TGFB2*). The best fit model for each gene was selected using MrModeltest 2.2 (Nylander, 2004) based on the Akaike information criterion (AIC), in conjunction with PAUP* (Swofford, 1998). Phylogenies were estimated using MrBayes 3.1.2 (Huelsenbeck and Ronquist, 2001) and RAxML (Stamatakis et al., 2008) for BI and ML, respectively. Two independent Bayesian runs of 20 million generations with four chains of Markov chain Monte Carlo (MCMC) each were performed. The first million generations were discarded as burn-in, after which trees were sampled every 500 generations. Chain convergence (Effective Sample Size – ESS values > 200) was checked using the likelihood plots for each run using Tracer 1.5 (http://beast.bio.ed.ac.uk/Tracer). The Potential Scale Reduction Factor was also used to check chain convergence and burn-in; values close to one indicate good convergence between runs (Gelman and Rubin, 1992). RAxML analysis was run under the GTRAC model; invariable sites and gamma distribution were estimated for each partition during the run. Node supports of the maximum likelihood analyses were estimated by 1000 bootstrap replications. In addition, we obtained trees separately in RAxML for mitochondrial (*ND3*, *ND2* and *cytb*) and nuclear (*G3PDH* and *TGFB2*)
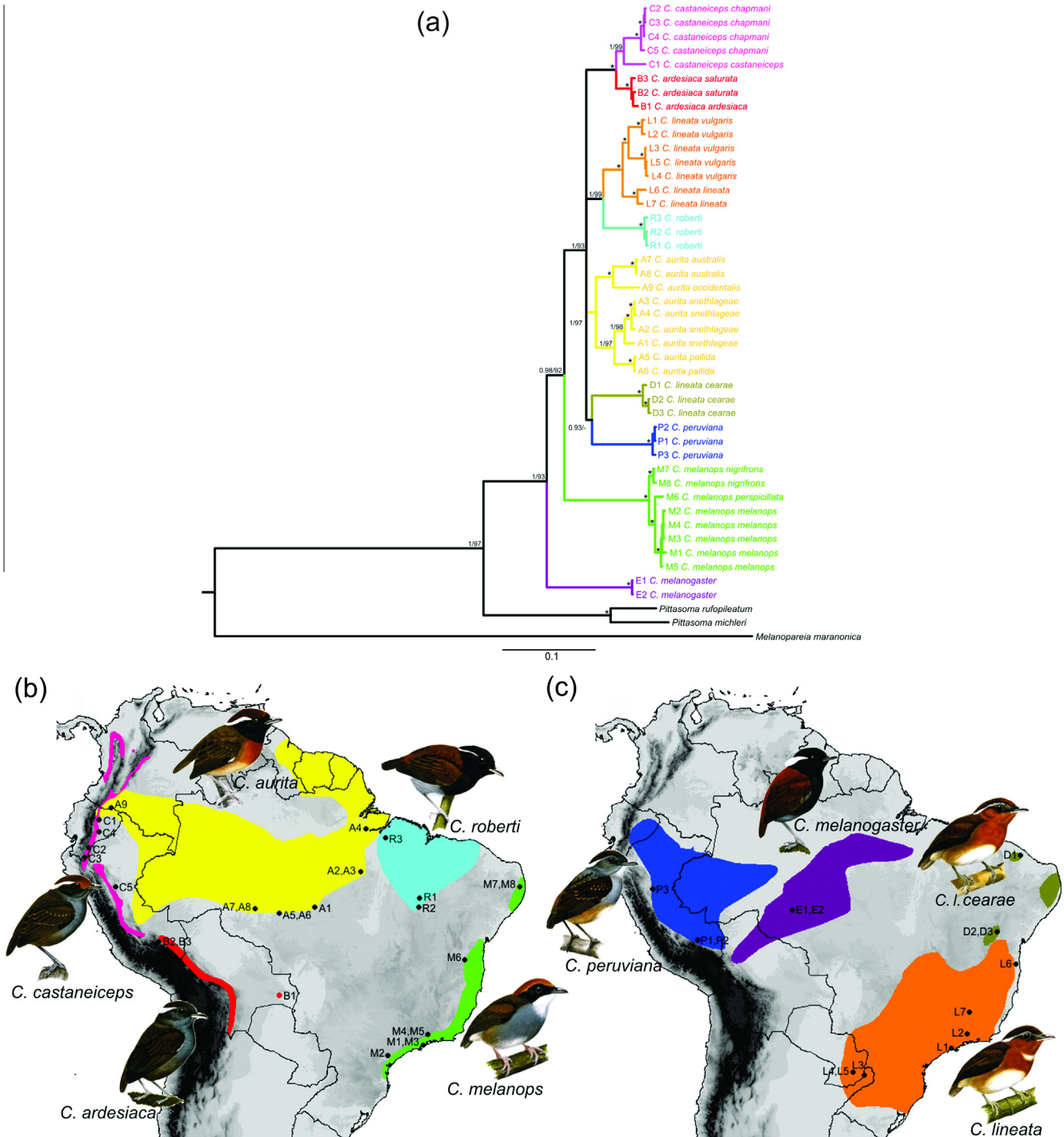
Fig. 1. (a) Phylogenetic relationships of Conopophagidae. The topology was obtained by Bayesian inference based on 3309 bp of mitochondrial and nuclear gene concatenated sequences. Node supports are posterior probabilities (PP) and bootstrap (BT) values for Bayesian inference and maximum likelihood, respectively. Asterisks indicate when both PP and BT were maximum (1.0 and 100, respectively). The colors and codes in the tree refer to the maps. (b and c) Maps with geographic distribution of *Conopophaga* species. Circles on the map indicate sampling sites and their codes correspond to the sequences in the tree. Species distributions are based on digital maps provided by Ridgely et al. (2003). The gradient of gray color in the map represents the elevation gradient (the darker the higher is the altitude). *Conopophaga* illustrations are courtesy of Lynx Edicions (Handbook of the birds of the world, Vol. 8, 2003). (For interpretation of the references to color in this figure legend, the reader is referred to the web version of this article.)

alignments. MrBayes and RAxML analyses were carried out at CIPRES Science Gateway (Miller et al., 2010).

2.3. Divergence time estimation

Divergence time estimates were obtained by implementing a Bayesian relaxed clock model in BEAST 1.7.4 (Drummond et al., 2012) based on a concatenated mitochondrial dataset as well as all genes concatenated, and using the CIPRES Science Gateway. We used relaxed clock with an uncorrelated lognormal distribution (Drummond et al., 2006) as indicated by hLRT tests, UPGMA starting tree and Yule process for both datasets. We considered the same partitions and models used in the phylogenetic reconstructions, as estimated in MrModeltest 2.2. As the fossil record of

New World suboscines is very sparse, we used two different strategies of calibration to obtain absolute divergence times: (i) concatenated dataset – a secondary calibration of the root of Conopophagidae family as estimated by Ohlson et al. (2013) of 20.05 Mya (95% confidence interval: 15.66–24.86) under a normal distributed prior; (ii) mitochondrial dataset – a mutation rate of mitochondrial genes (under a normal distributed prior) for birds of 1.05% (±0.05) per lineage per million years (Weir and Schluter, 2008). We performed two independent runs with each dataset with 100 million generations each, with parameters sampled every 10,000 steps and a burn-in of 10%. We checked for convergence between runs and analysis performance using Tracer 1.5, and accepted the results if ESS values were >200. The resulting trees were combined in TreeAnotator and the consensus species tree with the divergence times was visualized in FigTree 1.4 (http://tree.bio.ed.ac.uk/software/figtree/).

2.4. Ancestral area reconstruction

We used the package BioGeoBEARS (BioGeography with Bayesian Evolutionary Analysis in R Scripts'; Matzke 2013; http://cran.r-project.org/web/packages/BioGeoBEARS/index.html) to infer the ancestral areas for the *Conopophaga* clade. This package uses a maximum likelihood method similar to LAGRANGE (Ree et al., 2005; Ree and Smith, 2008). In this inference, ancestral areas are optimized onto internal nodes. BioGeoBEARS calculates maximum likelihood estimates of the ancestral states (range inheritance scenarios) at speciation events by modeling transitions between discrete states (biogeographical ranges) along phylogenetic branches as a function of time. It allows the use of the LAGRANGE DEC model (Dispersal Extinction Cladogenesis) and a new model called BioGeoBEARS DEC + J model (see Ree et al., 2005 and Matzke, 2013 for further details). Both models include two free parameters (d = dispersal and e = extinction), but DEC + J includes the additional parameter j that corresponds to founder event speciation. Likelihood values of these models were compared using Likelihood Ratio Test (LRT). We defined four geographical areas for the BioGeoBEARS analysis after considering the evidence available for historical relationships between relevant geographic areas in South America (Hoorn et al., 2010) and the distribution of *Conopophaga* taxa. These regions were as follows: Andes, South Amazonia, North Amazonia, and Atlantic Forest. Two of the most stable geological regions in South America are represented in these areas: Brazilian Shield (South Amazonia and Atlantic Forest), and Guiana Shield (North Amazonia). The ancestral area probability was computed for each node and subsequently plotted on the majority-rule chronogram using R scripts (available from P.-H.F. on request). We set the maximum number of areas at four.

2.5. Diversification rate analysis

We used R (R Development Core Team, 2012) with the APE and the LASER packages (Paradis et al., 2004; Rabosky, 2006) to calculate the diversification rate of genus *Conopophaga*. The analyses were computed on the maximum clade credibility tree and on 1000 phylogenies randomly sampled from the posterior distributions of trees (excluding the burn-in) in order to take into account the phylogenetic uncertainty. We kept only one lineage per species as delineated by our molecular dating results. We tested for constant diversification rates over time using both the γ statistic (Pybus and Harvey, 2000) and the maximum likelihood method of the AIC_{RC} (Rabosky, 2006). We obtained the null distribution for both estimations from 5000 simulated topologies of the same sample size. The sample size used (number of species; N = 11) was based on the results from the molecular species phylogeny. To test the effects of undetected or extinct species, we used three

further levels of total species richness, by assuming that the known number of species represents 75%, 50%, and 25% of the true number of species. The trees were simulated based on the assumed total species number, and tips were reduced to the number sampled in our phylogenies. All our simulations assumed that missing species were randomly distributed in the phylogeny. We assumed that our taxon sampling of *Conopophaga* is complete as all except two of the currently recognized subspecies were analyzed and most of these taxa were represented by samples from multiple sites. A strongly negative γ is associated with a decrease in diversification rates over time (rejection of constant diversification), whereas a positive value could represent constant or increasing diversification rates. We used a one-tailed test to detect significant negative γ values, which is considered conservative if extinction is nonzero (Pybus and Harvey, 2000). We subsequently fitted five maximum-likelihood diversification models; (i) the Yule model (constant speciation rate without extinction), (ii) a birth–death model (constant speciation rate and constant, nonzero extinction rate), (iii) a diversity-dependent diversification model with exponentially decreasing speciation, (iv) zero extinction rates, (v) a modified Yule model allowing for two different speciation rates with a breakpoint (Rabosky, 2006). The latter three represent models with rates that vary through time with a diversity-dependent diversification model with linearly decreasing speciation and zero extinction rates. The AIC_{RC} measure is computed as the difference in AIC values between the best rate-variable model and the best rate-constant model. The AIC_{RC} is positive if the best model is rate-variable. Significant positive AIC_{RC} values were implemented using a one-tailed test against the simulated null distributions (Rabosky, 2006).

Using GEIGER (Harmon et al., 2008) and apTreeshape packages (Bortolussi et al., 2006) we implemented two approaches to identify nodes that display significant shifts in diversification rates: the $\Delta 1$ statistic, which considers topological information only, and the relative cladogenesis test, which tests lineages within time slices along the whole chronogram for differences in the number of descendants (Nee et al., 1992).

3. Results

3.1. Phylogenetic inferences

We obtained a concatenated matrix of 3309 bp for most samples (46 individuals, including outgroup): 343 bp of *ND3*, 941 bp of *ND2*, 986 bp of *cytb*, 391 bp *G3PDH*, and 648 bp of *TGFB2*. Considering the ingroup only, there were 129, 382, and 357 variable sites in *ND3*, *ND2*, and *cytb*, respectively. No indels, unexpected stop codons, or ambiguous peaks in the electropherograms were found in these sequences, suggesting that they were of mitochondrial origin. In the nuclear intron sequences, we observed 59 and 36 variable sites in *G3PDH* and *TGFB2*, respectively. For the alignment of *G3PDH* we found five indels that varied between one to eight bp long. Three of these are congruent with the phylogenetic results: an indel of eight bp was shared by samples of *C. lineata vulgaris*, an indel of four bp was found only in *C. aurita australis*, an indel of one bp was shared only by samples of *C. melanogaster*, and another indel of one bp was found only in *C. ardesiaca*. The remaining indel of one bp was found in *C. l. cearae*, *C. melanogaster*, *C. melanops* and *C. roberti*, and its presence was not congruent with the phylogeny. We found three indels in *TGFB2* (two of six bp, and one of one bp); one indel of six bp was present in all samples of *C. melanops* and *C. melanogaster*, a six bp indel was shared between *C. aurita snethlageae* and *C. aurita pallida*, and a one bp indel was shared between *C. a. australis* and *C. a. occidetalis*. These indels in *TGFB2* were all congruent with the phylogenetic results (Fig. 1), thus providing additional support for these clades. All sequences were deposited in GenBank (accession numbers, *ND3*: KJ912712

– KJ912756; *ND2*: KJ912668 – KJ912711; *cytb*: KJ912627 – KJ912667; *G3PDH*: KJ912757 – KJ912794; *TGFB2*: KJ912795 – KJ912831).

The best fit models selected for each partition were as follows: GTR + I + Γ for *ND3* and *ND2*, HKY + I + Γ for *cytb*, GTR + I for *G3PDH*, and HKY + I for *TGFB2*. The phylogenies for both mitochondrial and concatenated datasets strongly supported the reciprocal monophyly of genera *Conopophaga* and *Pittasoma* (Fig. 1). Furthermore, all species were monophyletic with the exception of *C. lineata*, as *C. lineata cearae* did not cluster with *C. l. lineata* and *C. l. vulgaris* (Fig. 1). The BI tree recovered *C. l. cearae* as sister of *C. peruviana* (Fig. 1), but with low node support (posterior probability [PP] of 0.93). Also, the relationships of *C. l. ceareae* with other species could not be resolved in the ML phylogeny. The ML tree for the nuclear dataset recovered most species as monophyletic, but the relationships between them were poorly supported (not shown).

Two major clades were observed in the phylogeny: one comprising genus *Pittasoma*, and another, *Conopophaga* (Fig. 1). Within *Conopophaga*, three well supported major clades were recognized. A basal lineage was comprised by the southern Amazonian *C. melanogaster*, while the other cluster included a clade with *C. melanops* and another clade with all remaining *Conopophaga* species (Fig. 1). Basal relationships within this latter clade were poorly resolved and are best regarded as forming a polytomy. Nevertheless, some nodes in this clade showed strong support (Fig. 1): (i) *C. ardesiaca* as sister of *C. castaneiceps*; (ii) *C. lineata* as sister of *C. roberti*.

Our phylogenies also revealed most subspecies as monophyletic, but within *C. ardesiaca* the subspecies *C. a. saturata* was paraphyletic with respect to *C. a. ardesiaca*. Within *C. aurita* and *C. lineata* we also found deep divergences between subspecies (Fig. 1). The form *C. l. cearae* represents an independent lineage (see above). Our phylogenies also revealed genetic structure within *C. l. vulgaris*, with two clades that are congruent with a central (Fig. 1; L1 and L2) and a southern (Fig. 1; L3, L4 and L5) Atlantic Forest distribution. *C. aurita* exhibited a structured diversity in western Amazonia (*C. a. australis* and *C. a. occidentalis*) and eastern Amazonia (*C. a. snethlageae* and *C. a. pallida*). Also, in *C. melanops* three clades were recovered which correspond each to recognized subspecies (Fig. 1): *C. m. nigrifrons* (M7 and M8), *C. m. perspicillata* (M6), and *C. m. melanops* (M1, M2, M3, M4 and M5).

3.2. Divergence times

The absolute divergence times of the gnateaters generated by BEAST revealed an initial divergence of *Pittasoma* and *Conopophaga* during the early Miocene and the radiation within *Conopophaga* during the late Miocene (Fig. 2). Divergence time estimates for concatenated and mitochondrial datasets were very similar for all nodes within *Conopophaga*, and all 95% of high posterior densities (HPD) for node dates overlapped between these two estimations (Table 1). The oldest divergence was the split between *Pittasoma* and *Conopophaga* (~18 Mya; Fig. 2; Table 1). Within *Pittasoma*, the divergence between its two species was ~6 Mya (Fig. 2; Table 1). Within *Conopophaga*, the oldest divergence was the basal split between *C. melanogaster* and the remaining species (~10.5 Mya), whereas the most recent was the split between *C. ardesiaca* and *C. castaneiceps* (~3 Mya; Fig. 2; Table 1). In addition, comparatively old divergences (~6.5–1.5 Mya) were also found between subspecies in some of the polytypic species (i.e. *C. aurita*, *C. lineata*, and *C. castaneiceps*).

3.3. Ancestral distribution of Conopophaga

The model that best fitted the phylogenetic reconstruction of *Conopophaga* was DEC + J (ln *L* = −40.5), while DEC (ln *L* = −44.1)

was less likely (LRT = 7.2, *p* < 0.05). The most likely ancestral area reconstruction is given in Fig. 2 (see Fig. S1 in supplementary material for node pie charts likelihoods of ancestral areas). This biogeographic reconstruction indicated a South Amazon plus Atlantic Forest origin, which comprises one of the geologically most stable areas in South America, the Brazilian Shield. Our analysis suggested a vicariant event during the Late Miocene, with *C. melanogaster* and *C. melanops* in opposite sides of the shield, in the southern Amazon and the Atlantic Forests. The most likely origin for the clade containing the remaining *Conopophaga* species (node D), except *C. melanogaster*, was the Atlantic Forest. From this area, the clade that holds the remaining *Conopophaga* species seems to have recolonized the Amazon area. Other putative major events involved: (i) the dispersal of the ancestor of *C. castaneiceps* and *C. ardesiaca* (node I) toward the Andes and their speciation possibly due to the orogenic changes in the eastern Andean region; (ii) two vicariant events between the Atlantic Forest and the Amazon involving the splits between *C. lineata* and *C. roberti* (node H), and *C. l. cearae* and *C. peruviana* (node F); (iii) the range expansion of *C. aurita* to the North Amazon (node G). However, it is noteworthy to remind that this ancestral area reconstruction should be interpreted with caution, as some nodes were poorly resolved in our phylogenetic reconstructions (Fig. 1).

3.4. Diversification rate

The lineage-through-time plot for *Conopophaga* (Fig. 3) levelled off slightly after an initial rapid diversification, generating an apparent diversity-dependent pattern. Both the *γ* statistic and AIC$_{RC}$ indicated a decrease of diversification rate through time and the diversity dependent model being the best model for subspecies diversification (Tables 2 and 3). The observed *γ* and AIC$_{RC}$ of the maximum clade credibility tree for *Conopophaga* was significantly lower than expected if diversification were constant through time even if the tree only included 50% of the true diversity. We did not identify any shifts in diversification rates in *Conopophaga* (Delta 1 or RRT test).

4. Discussion

4.1. Origin and diversification of the gnateaters in South America

Although Conopophagidae represents one of the oldest lineages among the New World suboscines (~41 Mya; Ohlson et al., 2013), this family has very few species when compared to other lineages of similar age within the New World suboscines, such as the Thamnophilidae, Furnarioidea and Tyrannoidea groups. This suggests that extinction of deep branches may have occurred, as was also observed by the imbalance of branching in many parts of the Suboscines chronogram by Ohlson et al. (2013). Besides, it is worth mentioning that the radiation of the *Conopophaga* clade started rather recently (upper Miocene; ~11 Mya; Fig. 2). Thus, *Pittasoma* seems to be a possible relictual lineage that diverged during the late Oligocene to early Miocene (Fig. 2; Table 1). Moreover, the imbalanced phylogeny of the Thamnophiloidea superfamily, which contains old and species-poor genera, such as *Melanopareia* (Melanopareiidae), *Pittasoma*, and *Euchrepomis* (Euchrepominae), seems to suggest a relictual pattern, where extinctions may have put a veil over the early radiation of tracheophone suboscines.

Despite this, the predominance of taxa representing deep Thamnophiloidea lineages in the Eastern Brazilian-Andean area (Irestedt et al., 2002) may suggest an origin in this region. *Conopophaga* species are mainly distributed within the Brazilian Shield area and along the western margin of the Amazon Basin, corresponding to an Eastern Brazilian-Andean biogeographical pattern
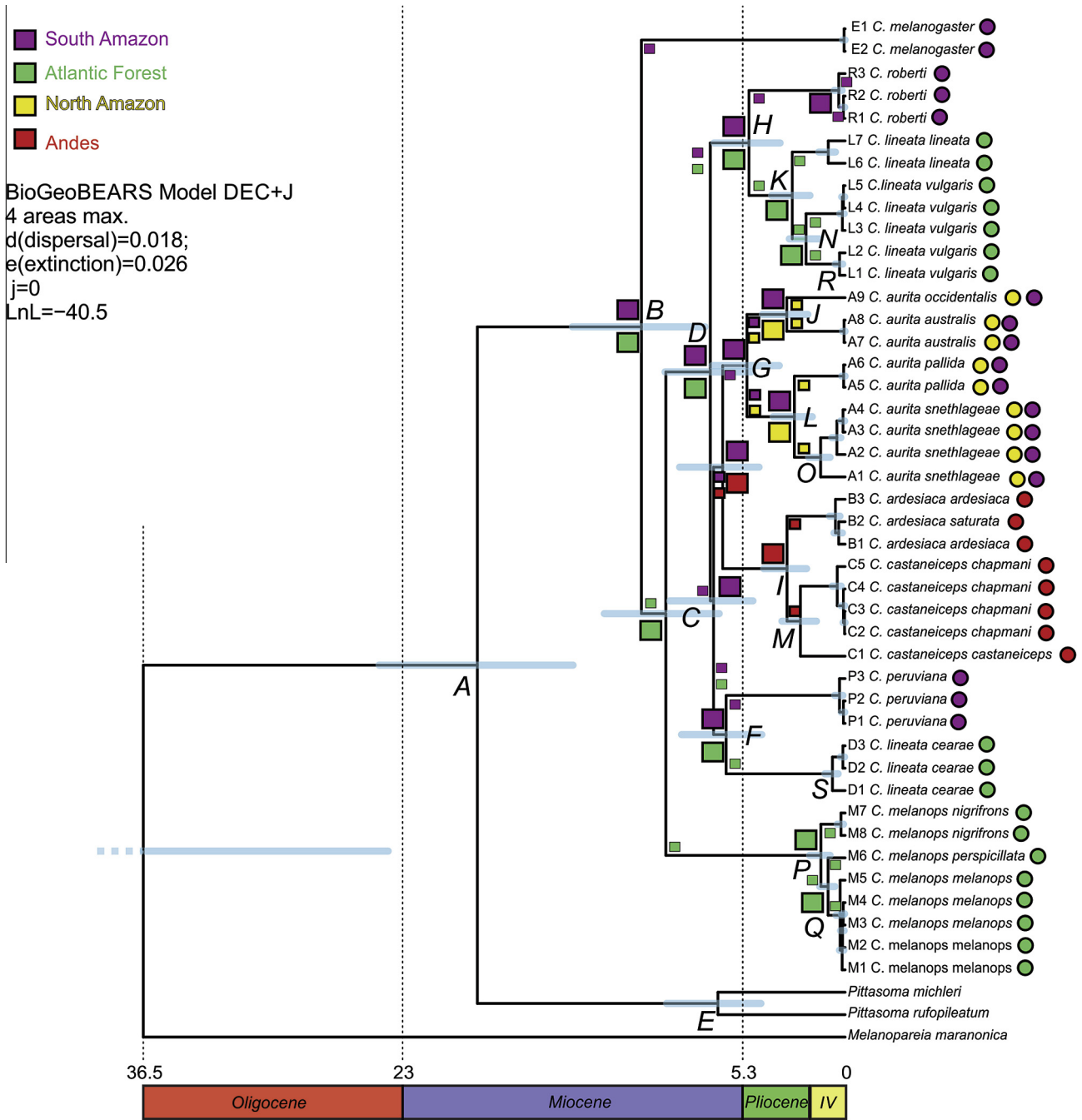
Fig. 2. Chronogram with divergence times for Conopophagidae generated by BEAST and ancestral distribution for *Conopophaga* provided by BioGeoBEARS. Letters at the nodes are divergence times between clades according to Table 1. Bars on the nodes represent 95% of high posterior density of divergence times. The most probable area states are shown at left of the node; note that these are the most probable states at each node and corner (corners represent the states just after speciation and are represented by a smaller square). The DEC + J model shows much less uncertainty in ancestral states, favors ancestors with single continental ranges, and confirms the progression of taxa from the South Amazonia and Atlantic Forest to other area (Andes and North Amazonia). The color code at tips represents the current distribution of taxa. Legends: Andes = red, South Amazon = magenta, North Amazon = yellow and Atlantic Forest = green. Ranges that are combinations of these two areas are represented by two squares of different colors. (For interpretation of the references to color in this figure legend, the reader is referred to the web version of this article.)

(Silva, 1995). It is in accordance with our ancestral area reconstruction, which indicated that the ancestor of the genus was probably distributed around the Brazilian Shield (Fig. 2: South Amazon plus Atlantic Forest areas). Thus, only the widespread Amazonian *C. aurita* extends north of the Amazon, in Amapá and the Guianas, and up to Rio Negro, which could represent an expansion before the establishment of the Amazonas river drainage channel to the Atlantic Ocean in the Plio-Pleistocene (Campbell et al., 2006; Latrubesse et al., 2010). Notwithstanding, as our analyses do not include samples of *C. aurita* from north of the Amazon River, our

statement of a Brazilian Shield origin for *Conopophaga* could change if the population from that region would not cluster with any of the lineages of *C. aurita* recovered in our study.

The dating of the split between the Eastern Brazilian-Andean *Conopophaga* and *Pittasoma* of the Chocó region (Fig. 2: node A, ~18.8 Mya) agrees with the early mountain building in the northern Andes (Hoorn et al., 2010: 23–10 Mya), when the biota of the northern proto-Andean peninsula (corresponding to the Chocó region) was isolated from that of Amazonia. The young divergence between *P. rufopileatum* and *P. michleri* can be attributed to a

Table 1
Divergence times and confidence intervals [95% of high posterior density (HPD)] in millions of years (Mya) between major clades of Conopophagidae. Node letters follow Fig. 2.

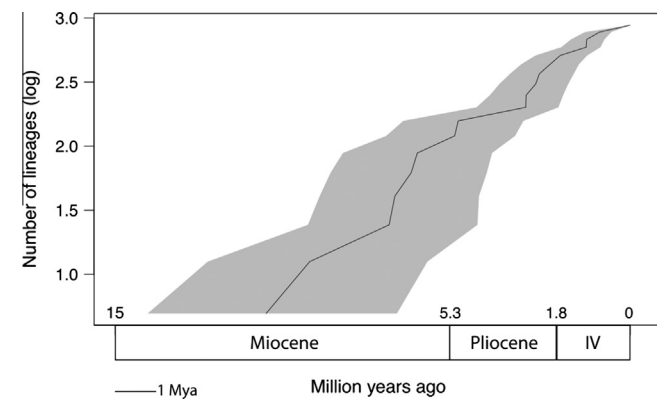| Node	Age Mya (95% of HPD)	
	Concatenated	Mitochondrial
A	18.88 (24.26–14.16)	18.00 (21.59–14.42)
B	10.56 (14.20–7.48)	11.12 (13.19–9.23)
C	9.27 (12.53–6.55)	9.73 (11.38–8.08)
D	6.97 (9.37–4.89)	7.80 (8.45–6.26)
E	6.62 (9.30–4.38)	5.43 (7.11–3.90)
F	6.18 (8.52–4.34)	–
G	5.09 (6.93–3.43)	5.24 (6.24–4.32)
H	4.98 (6.83–3.39)	5.12 (6.14–4.39)
I	3.03 (4.24–2.01)	3.14 (3.85–2.45)
J	3.04 (4.31–1.94)	3.27 (4.06–2.38)
K	2.74 (3.83–1.83)	2.85 (3.49–2.25)
L	2.65 (3.75–1.71)	2.64 (3.30–1.99)
M	2.33 (3.29–1.50)	2.44 (3.07–1.83)
N	2.04 (2.91–1.29)	2.10 (2.65–1.54)
O	1.29 (1.90–0.78)	1.24 (1.65–0.87)
P	1.27 (1.89–0.78)	1.24 (1.62–0.90)
Q	0.89 (1.32–0.54)	0.9 (1.20–0.60)
R	0.89 (1.38–0.51)	0.88 (1.24–0.56)
S	0.67 (1.06–0.37)	0.7 (0.99–0.42)

Fig. 3. Lineage through time plot (LTT plot) of *Conopophaga* based on the Conopophagidae timetree generated by BEAST.

Table 3
Maximum likelihood analysis of diversification rates in the *Conopophaga* phylogeny. Rate-constant and rate-variable models of diversification fit to the ultrametric phylogeny. Model names as in laser (Rabosky, 2006). AIC scores are provided for each of the empirical LTTs. AIC scores from the rate-constant and rate-variable models providing the best fit are noted with bold, as well as AIC values and *P*-values.

Model	LH	AIC	dAIC
pureBirth	**−9.47**	**20.93**	**1.23**
bd	−9.47	22.93	3.23
DDL	**−7.85**	**19.71**	**0.00**
DDX	−8.52	21.05	1.34
yule2rate	−7.9	21.79	2.08

Pebas and Acre wetlands systems were filled with sediment (Figs. 2 and 4) (Aleixo and Rosseti, 2007; and see Latrubesse et al., 2010). Thus, Conopophagidae data add to the general diversification pattern in the Thamnophiloidea, with species-poor clades of relatively restricted geographical distributions, until the fairly recent phylogenetic expansion in the *Conopophaga* clade (Figs. 2 and 4). In the late Miocene to Pliocene the remarkable northward mountain building of the Andes (Hoorn et al., 2010) allowed *Conopophaga* to colonize (disperse) and diversify along the forest-clad Andean foothill ridges (Figs. 2 and 4). Even during that period, two independent lineages of gnateaters (*C. lineata* [*vulgaris* plus *lineata* forms] and *C. l. cearae*) diversified in the Atlantic Forest (Figs. 2 and 4), and suggest a historical connection with the Amazon forest (Batalha-Filho et al., 2013).

The diversification analysis indicated a best topological-fit to a diversity-dependent model (γ and AIC_{RC}; Tables 2 and 3) and a slight decrease of the diversification rates within *Conopophaga* (see lineage through time plot in Fig. 3). However, such decrease of diversification in *Conopophaga* is not in accordance with other Neotropical groups that exhibited a pattern of constant diversification rate through the late Tertiary to Quaternary (Derryberry et al., 2011; d'Horta et al., 2013; Patel et al., 2011). Our diversification result thus corroborates the relictual status of *Conopophaga*, which seems to have filled a limited ecological space in the South America (a diversity-dependent pattern). This pattern might also be linked to the very specialize ecology of *Conopophaga*, which have in consequence restricted speciation opportunity compared to other New World suboscines. Moreover, we did not detect any significant shift in the diversification rate (see results section), a fact against a potential growing scenario. In such a growing scenario, the origin of Neotropical biota cannot be attributed to only one or few events during key time intervals (Rull, 2011a). This result reinforced the idea that *Conopophaga* represent an old and very specialize lineage, less prone to important diversification compared to its New World suboscines relatives. Despite this poor diversity, our Neotropical *Conopophaga* phylogeny provides a good biogeographical model shaped by a complex sequence of landscape changes through the Miocene and the Quaternary (see previous discussion part, Fig. 4). These can include Andes uplift (Hoorn et al., 2010), marine incursions (Antonelli and Sanmartín, 2011; Hoorn et al., 2010), Plio-Pleistocene formation of flat depositional basins with the
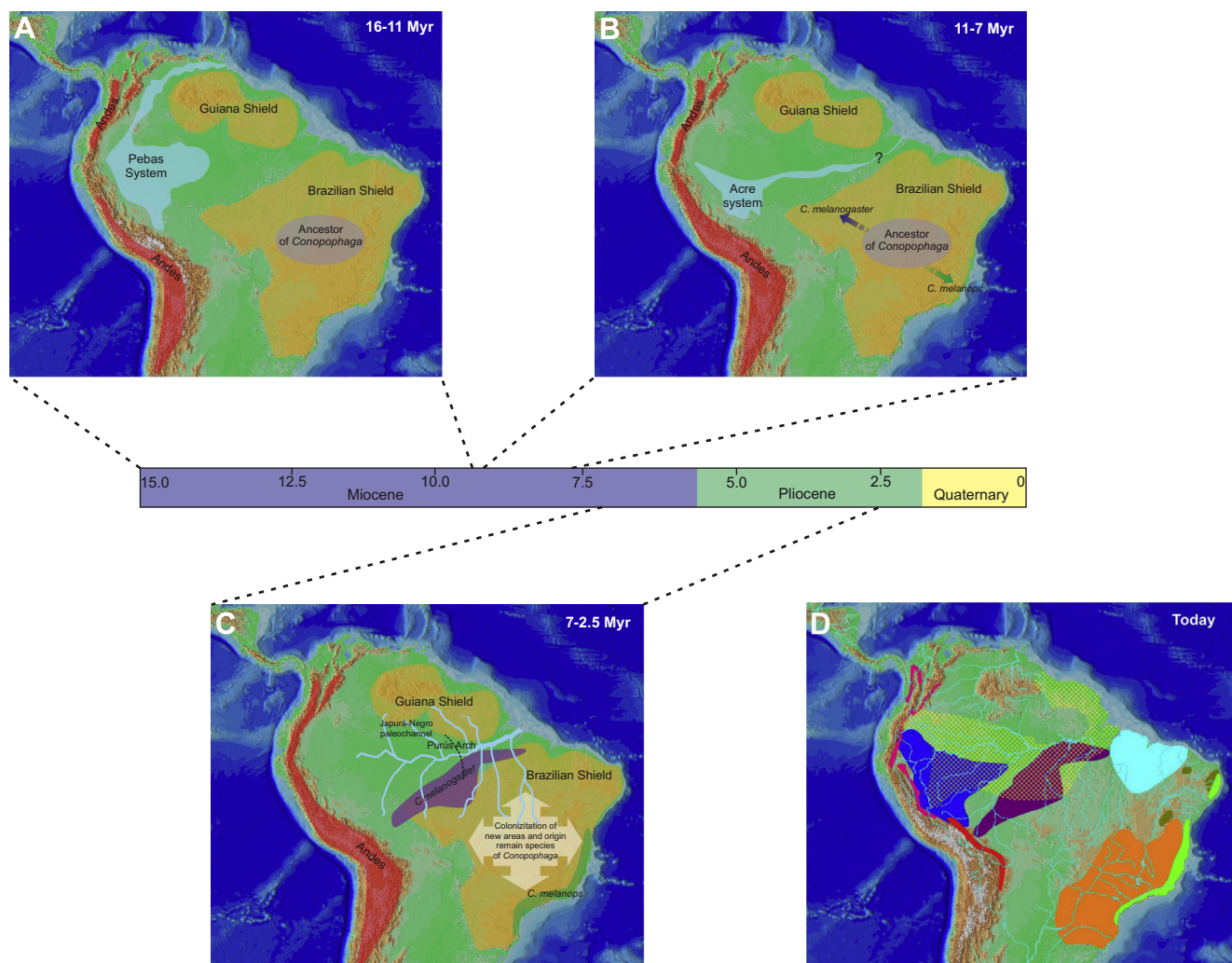
recent dispersion after the closure of the Panama isthmus by an ancestor of *P. michleri*. This is supported by the confidence intervals of our time estimates (Fig. 2; Table 1) and is in accordance with the estimated geological period of the Panama isthmus closure (~4–3 Mya; Coates and Obando 1996; Kirby et al., 2008). Other passerines exhibited a similar pattern of dispersion (Smith and Klicka, 2010; Weir et al., 2009).

The ancestral area reconstruction of *Conopophaga* could indicate an origin along the margins of the Brazilian Shield (Figs. 2 and 4). In our biogeographic inference the ancestral lineage of *Conopophaga* seems to have its distribution centered on the Brazilian Shield and started to colonize the western Amazonia basin only as the

Table 2
Test of constancy of diversification rates using the γ and $\Delta AICRC$ statistics. Observed statistics are for the maximum clade credibility (MCC) trees; *P*-values (significant at ≤ 0.05 is in bold) are shown for the MCC tree and the 95 percentile of a random sample (1000 trees) from the posterior distribution of trees. The *P*-values were generated from simulated null distributions of 5000 trees for each taxon and each of the assumed total species numbers. Simulations all accounted for the number of species not sampled in our phylogenies, and assumed that all species were known (100%), or that only 75%, 50%, and 25% were known, respectively.

	P-values									
	Observed statistic		100% known		75%		50%		25%	
	MCC	95th	MCC	95th	MCC	95th	MCC	95th	MCC	95th
GammaMCC	−1.34	−1.34	**0.04**	0.06	**0.05**	0.09	0.16	0.27	0.38	0.52
dAICrc	1.23	1.27	0.18	0.27	0.09	0.16	0.27	0.4	0.46	0.6

Fig. 4. Hypothesized spatiotemporal paleoscenarios of evolution of genus *Conopophaga*, with paleomaps created following Hoorn et al. (2010). (A) Middle Miocene: Amazonia west of the Purus Arch dominated by wetlands (Pebas system); ancestor of genus *Conopophaga* possibly occurred in the Brazilian Shield region. (B) Late Miocene: accelerated mountain building in central and northern Andes. Initial establishment of the transcontinental Amazon basin. Western Amazonia still holds wetlands (Acre system), but with nutrients from wetlands system flowing to the eastern Amazonia. Origin of *C. melanogaster* and *C. melanops* in the southeastern Amazonia and Atlantic Forest, respectively. (C) Late Miocene to Pliocene: closure of Panamá Isthmus, establishment of modern drainage of Amazon river (Late Pliocene to Pleistocene; Campbell et al., 2006; Latrubesse et al., 2010) and final phase of Andean uplift. The Purus arch is limiting eastward the wetland system from the west Amazonia until 6 Mya (Latrubesse et al., 2010). Draining of the wetlands from western Amazonia and subsequent expansion of forests to this region. Origin and diversification of the remaining species of genus *Conopophaga* in Amazonia, Atlantic Forest, and cloud forests of Andes. (D) Current scenario: the modern Amazon river established and Andean cordillera uplifted. All currently extant *Conopophaga* species diversified. Color of species distribution follow figure. (For interpretation of the references to color in this figure legend, the reader is referred to the web version of this article.).

Amazonian megafans and establishment of the east-draining Amazon river (Ribas et al., 2012), as well as Pleistocene climatic-vegetational changes (Carnaval et al., 2009; Cheng et al., 2013).

4.2. Diversification of the Atlantic Forest lineages

Three independent evolutionary lineages of *Conopophaga* are endemic to the Atlantic Forest: *C. melanops*, *C. lineata*, and *C. l. cearae* (Fig. 1). *C. melanops* is the oldest lineage, and diverged from all other species of *Conopophaga* in the late Miocene (Fig. 2; Table 1). Recent studies showed that the Atlantic Forest holds ancient lineages that date from the mid-Tertiary for birds (Derryberry et al., 2011), mammals (Fabre et al., 2013; Galewski et al., 2005) and frogs (Fouquet et al., 2012). *C. lineata* and *C. l. cearae* originated around the late Miocene to early Pliocene (Fig. 2; Table 1) and have Amazonian sister species, in accordance with hypotheses of historical connections between Amazonia and Atlantic Forest biota (Batalha-Filho et al., 2013; Cheng et al., 2013; Costa, 2003; Willis, 1992).

Our data confirmed the Atlantic Forest diversity, and revealed several cryptic intra-specific lineages. It is noteworthy to highlight distinct diversification patterns of *C. melanops*, *C. lineata* and *C. l. cearae*. Indeed, *C. lineata* exhibited higher mean intra-specific uncorrected genetic distance based on mtDNA data (*C. lineata*, 3.51%; *C. melanops*, 0.72%; *C. l. cearae*, 0.58%), as well as longer intra-specific branch lengths (Figs. 1 and 2). In *C. lineata* the first divergence occurred during the late Pliocene to early Pleistocene, whereas in *C. melanops* and *C. l. cearae* the split took place in the Pleistocene. Interestingly, *C. lineata* and *C. melanops* have similar latitudinal distribution in the Atlantic Forest (Ridgely and Tudor, 1994; Fig. 1) and similar geographic structure (two components: one in the north and one in the south), but they exhibited distinct temporal splitting patterns (Fig. 2; Table 1). This incongruence on the temporal patterns could be related to the different elevation distributions: *C. lineata* inhabits upland forest (500–2400 m) while *C. melanops* is mainly found in lowland forest (up to 800 m) (Whitney, 2003). Lowland and upland regions in the Atlantic Forest

seem to have been affected by the Quaternary climate changes in different ways. In general, species of lowland forests show strong signatures of the effect of the last glacial maximum (Carnaval et al., 2009), whereas some upland organisms do not (Amaro et al., 2012; Batalha-Filho et al., 2012).

4.3. Diversification in the Amazon basin

While the first split of Amazonian gnateaters, which gave rise to *C. melanogaster*, is of mid-Miocene age, the other three splits occurred through the late Miocene to early Pliocene (Fig. 2; Table 1). As in the Atlantic Forest, the four Amazonian species (*C. melanogaster*, *C. aurita*, *C. peruviana*, and *C. roberti*) represent independent evolutionary lineages in the phylogeny (Fig. 1). However, it is important to note that, because of the poor resolution of some deep branches, some Amazonian species, such as *C. aurita* and *C. peruviana*, could in fact present a sister taxa relationship. The lack of monophyly of the Amazonian species was also observed in other forest birds, such as *Brotogeris* (Ribas et al., 2009) and *Sclerurus* (d'Horta et al., 2013). Thus, it is possible that the Amazonian biota may have multiple origins (Ribas et al., 2009) and *Conopophaga* may represent a new example of expansion from the East Brazilian-Andean elevated land surfaces.

Intra-specific diversification within Amazonia was detected only in the geographically widespread *C. aurita* (Fig. 1), which also shows the largest number of recognized subspecies (Whitney, 2003). The most basal divergence within *C. aurita* dates back to late Miocene to early Pliocene (Fig. 2; Table 1), and divides western and eastern Amazonian subspecies. Within these two groups further diversification took place in the Pliocene (Figs. 1 and 2). Given the possible origin of *Conopophaga* in the Brazilian Shield, we might assume a past expansion of *C. aurita* from this area before the final establishment of the Amazonian drainage channel to the Atlantic Ocean (through Late Miocene and Pliocene), and when the Japurá-Negro palaeochannel formed the northern fan margin of the central Amazon basin (Wilkinson et al., 2010). Further studies with a denser taxon sampling, including samples from the north of the Amazon River are needed to understand the phylogeographical structure of *C. aurita*.

4.4. Uplift of the Andes and diversification of gnateaters

The Andean species, *C. castaneiceps* and *C. ardesiaca*, form a monophyletic group with corresponding northern and central clades, respectively (Fig. 1). The Andean clade originated around the Late Miocene (Fig. 2), and the split might be related to the transitions between the lowland Amazon and the Andes (Upham et al., 2013). Divergence between Andean species occurred in the Pliocene (Fig. 2; Table 1). They overlap marginally in Cuzco, eastern Peru (Schulenberg et al., 2010), in a region with many species replacements, in the transition between the perhumid tropical Andes and the more seasonal "yungas" forest of eastern Peru and Bolivia (Bonaccorso, 2009; Gutiérrez-Pinto et al., 2012; Isler et al., 2012). We also detected divergent lineages in *C. castaneiceps* that split in the late Pliocene (Fig. 1 and 2). This pattern of diversification in the Andes is possibly correlated to the mountain building pattern of the Cordillera, that follows a south to north orogeny (Hoorn et al., 2010), and is in accordance with the rate of cladogenesis observed in other avian groups (Chaves et al., 2011; Ribas et al., 2007).

4.5. Systematics

In this study we provided the first comprehensive molecular phylogeny of the Neotropical gnateaters. Our phylogeny strongly supported both *Conopophaga* and *Pittasoma* as reciprocally mono-

phyletic lineages (Fig. 1), and also provided evidence for the taxonomic revision of *Conopophaga*. Even though relationships within *Conopophaga* were not fully resolved (Fig. 1), nine clades were well supported, including all previously recognized species and a paraphyletic relationship in *C. lineata*. The phylogeny placed the Andean taxa *C. castaneiceps* and *C. ardesiaca* as sister species, while the Atlantic Forest species were not monophyletic (Fig. 1). The form *cearae* has, until now, been recognized as a subspecies of *C. lineata*, based on plumage phenotypes (Whitney, 2003), but our results strongly suggests *C. l. cearae* as a separate species, and our Bayesian concatenated phylogeny recovered it as sister of *C. peruviana*, although with low support (0.93 of PP). Better genetic and geographical sampling of the disjunct geographical populations of *C. l. cearae* (in northern Chapada Diamantina, patches of forest amidst dry Caatinga locally known as *Brejos de Altitude*, and northern São Francisco River) may help to reveal ancient connections between Amazonia and the Atlantic Forest. The similarities in plumage between *C. lineata* and *C. (lineata) cearae* could be the result of retention of ancient polymorphism or parallel evolution, as these species share very similar plumage phenotypes.

We also observed genetic structure in four species (Fig. 1): *C. melanops*, *C. castaneiceps*, *C. lineata*, and *C. aurita*. As some of these clades are phenotypically and vocally diagnosable (Whitney, 2003), a detailed taxonomic revision of the genus may support that several of these subspecies also could be ranked as full species. In addition, further phylogeographic studies of these species with dense population sampling will help to comprehend the geographic variation in these taxa.

4.6. Conclusions

Our analyses of the diversification of the Conopophagidae family provided an additional scenario for the evolution in *Terra Firme* forest across tropical South America. The spatio-temporal pattern may reflect an evolutionary history influenced by several independent external events such as the Andean uplift (Hoorn et al., 2010), marine incursions (Antonelli and Sanmartín, 2011), paleoclimatic events (Carnaval et al., 2009; Cheng et al., 2013) as well as river formation (Ribas et al., 2012). Nevertheless, it is intriguing to observe that the *Conopophaga* clade diversified so recently. Apparently this diversification took place only within elevated/erosional landscapes, primarily south of the Amazon river, and outside the flat sedimentary parts of the wetlands and megafans of the western and central Amazon basin. Other old South American radiations took place within the Brazilian and Guiana shields, with recent Plio-Pleistocene radiation driven by wetland dynamics within the basin. However, *Conopophaga* may have been geographically more limited and did not show the same strong radiation (driven by river barriers) within the floodplains (with some exception for *C. aurita*).

Therefore, the origin of the Neotropical region biota seems to be a mosaic of many complex evolutionary scenarios (Rull, 2013), and as more studies become available more detailed scenarios may arise, and a more complete history will be elucidated in the future.

Appendix A. Supplementary material

Supplementary data associated with this article can be found, in the online version, at http://dx.doi.org/10.1016/j.ympev.2014.06.025.

References

Aleixo, A., Rosseti, D.F., 2007. Avian gene trees, landscape evolution, and geology: towards a modern synthesis of Amazonian historical biogeography? J. Ornithol. 148 (Suppl 2), S443–S453.

Amaro, R.C., Carnaval, A.C., Yonenaga-Yassuda, Y., Rodrigues, M.T., 2012. Demographic processes in the montane Atlantic rainforest: molecular and cytogenetic evidence from the endemic frog *Proceratophrys boiei*. Mol. Phylogenet. Evol. 63, 880–888.

Antonelli, A., Nylander, J.A.A., Persson, C., Sanmartín, I., 2009. Tracing the impact of the Andean uplift on Neotropical plant evolution. Proc. Natl. Acad. Sci. USA 106, 9749–9754.

Antonelli, A., Sanmartín, I., 2011. Why are there so many plant species in the Neotropics? Taxon 60, 403–414.

Batalha-Filho, H., Cabanne, G.S., Miyaki, C.Y., 2012. Phylogeography of an Atlantic Forest passerine reveals demographic stability through the last glacial maximum. Mol. Phylogenet. Evol. 65, 892–902.

Batalha-Filho, H., Fjeldså, J., Fabre, P.H., Miyaki, C.Y., 2013. Connections between the Atlantic and the Amazonian forest avifaunas represent distinct historical events. J. Ornithol. 154, 41–50.

Bonaccorso, E., 2009. Historical biogeography and speciation in the Neotropical highlands: molecular phylogenetics of the jay genus *Cyanolyca*. Mol. Phylogenet. Evol. 50, 618–632.

Bortolussi, N., Durand, E., Blum, M., Francois, O., 2006. ApTreeshape: statistical analysis of phylogenetic tree shape. Bioinformatics 22, 363–364.

Bruford, M.W., Hanotte, O., Brookfield, J.F.Y., Burke, T., 1992. Single-locus and multilocus DNA fingerprinting. In: Hoelzel, A.R. (Ed.), Molecular Genetic Analysis of Populations – A Practical Approach. IRL Press, New York, pp. 287–336.

Bush, M.B., de Oliveira, P.E., 2006. The rise and fall of the refugial hypothesis of Amazonian speciation: a paleoecological perspective. Biot. Neotrop. 6, 1–17.

Campbell Jr., K.E., Frailey, C.D., Romero-Pittman, L., 2006. The Pan-Amazonian Ucayali Peneplain, late Neogene sedimentation in Amazonia, and the birth of the modern Amazon River system. Palaeogeogr. Palaeoclimatol. Palaeoecol. 239, 166–219.

Carnaval, A.C., Moritz, C., 2008. Historical climate modeling predicts patterns of current biodiversity in the Brazilian Atlantic Forest. J. Biogeogr. 35, 1187–1201.

Carnaval, A.C., Hickerson, M.J., Haddad, C.F.B., Rodrigues, M.T., Moritz, C., 2009. Stability predicts genetic diversity in the Brazilian Atlantic Forest hotspot. Science 323, 785–789.

Chaves, J.A., Weir, J.T., Smith, T.B., 2011. Diversification in *Adelomyia* hummingbirds follows Andean uplift. Mol. Ecol. 20, 4564–4576.

Cheng, H., Sinha, A., Cruz, F.W., Wang, X., Edwards, R.L., d'Horta, F.M., Ribas, C.C., Vuille, M., Scott, L.D., Auler, A.S., 2013. Climate change patterns in Amazonia and biodiversity. Nat. Commun. 4, 1411.

Coates, A.G., Obando, J.A., 1996. The geologic evolution of the Central American Isthmus. In: Jackson, J., Budd, A.F., Coates, A.G. (Eds.), Evolution and Environment in Tropical America. University of Chicago Press, Chicago, pp. 21–56.

Colinvaux, P.A., de Oliveira, P.E., Bush, M.B., 2000. Amazonian and Neotropical plant communities on glacial time scales: the failure of the aridity and refuge hypothesis. Quaternary Sci. Rev. 19, 141–169.

Costa, L.P., 2003. The historical bridge between the Amazon and the Atlantic forest of Brazil: a study of molecular phylogeography with small mammals. J. Biogeogr. 30, 71–86.

Derryberry, E.P., Claramunt, S., Derryberry, G., Chesser, R.T., Cracraft, J., Aleixo, A., Pérez-Emán, J., Remsen, J.V., Brumfield, R.T., 2011. Lineage diversification and morphological evolution in a large-scale continental radiation: the Neotropical ovenbirds and woodcreepers (Aves: Furnariidae). Evolution 65, 2973–2986.

d'Horta, F.M., Cuervo, A.M., Ribas, C.C., Brumfield, R.T., Miyaki, C.Y., 2013. Phylogeny and comparative phylogeography of (Aves: Furnariidae) reveal constant and cryptic diversification in an old radiation of rain forest understorey specialists. J. Biogeogr. 40, 37–49.

Drummond, A.J., Ho, S.Y.W., Phillips, M.J., Rambaut, A., 2006. Relaxed phylogenetics and dating with confidence. PLoS Biol. 4, e88.

Drummond, A.J., Suchard, M.A., Xie, D., Rambaut, A., 2012. Bayesian phylogenetics with BEAUti and the BEAST 1.7. Mol. Biol. Evol. 29, 1969–1973.

Fabre, P.-H., Galewski, T., Tilak, M.-K., Douzery, E.J.P., 2013. Diversification of South American spiny rats (Echimyidae): a multigene phylogenetic approach. Zool. Scr. 42, 117–134.

Fernandes, A.M., Wink, M., Aleixo, A., 2012. Phylogeography of the chestnut-tailed antbird (*Myrmeciza hemimelaena*) clarifies the role of rivers in Amazonian biogeography. J. Biogeogr. 39, 1524–1535.

Fouquet, A., Recoder, R., Teixeira Jr., M., Cassimiro, J., Amaro, R.C., Camacho, A., Damasceno, R., Carnaval, A.C., Moritz, C., Rodrigues, M.T., 2012. Molecular phylogeny and morphometric analyses reveal deep divergence between Amazonia and Atlantic Forest species of *Dendrophryniscus*. Mol. Phylogenet. Evol. 62, 826–838.

Galewski, T., Mauffrey, J.F., Leite, Y.L., Patton, J.L., Douzery, E.J., 2005. Ecomorphological diversification among South American spiny rats (Rodentia; Echimyidae): a phylogenetic and chronological approach. Mol. Phylogenet. Evol. 34, 601–615.

Gelman, A., Rubin, D., 1992. Inference from iterative simulation using multiple sequences. Stat. Sci. 7, 457–511.

Gutiérrez-Pinto, N., Cuervo, A.M., Miranda, J., Pérez-Emán, J.L., Brumfield, R.T., Cadena, C.D., 2012. Non-monophyly and deep genetic differentiation across low-elevation barriers in a Neotropical montane bird (*Basileuterus tristriatus*; Aves: Parulidae). Mol. Phylogenet. Evol. 64, 156–165.

Haffer, J., 1969. Speciation in Amazonian forest birds. Science 165, 131–137.

Harmon, L.J., Weir, J.T., Brock, C.D., Glor, R.E., Challenger, W., 2008. GEIGER: investigating evolutionary radiations. Bioinformatics 24, 129–131.

Higgins, D., Thompson, J., Gibson, T., Thompson, J.D., Higgins, D.G., Gibson, T.J., 1994. CLUSTAL W: improving the sensitivity of progressive multiple sequence alignment through sequence weighting, position-specific gap penalties and weight matrix choice. Nucleic Acids Res. 22, 4673–4680.

Hoorn, C., Wesselingh, F.P., ter Steege, H., Bermudez, M.A., Mora, A., Sevink, J., Sanmartín, I., Sanchez-Meseguer, A., Anderson, C.L., Figueiredo, J.P., Jaramillo, C., Riff, D., Negri, F.R., Hooghiemstra, H., Lundberg, J., Stadler, T., Särkinen, T., Antonelli, A., 2010. Amazonia through time: Andean uplift, climate change, landscape evolution, and biodiversity. Science 330, 927–931.

Hoorn, C., Mosbrugger, V., Mulch, A., Antonelli, A., 2013. Biodiversity from mountain building. Nat. Geosci. 6, 154.

Huelsenbeck, J.P., Ronquist, F., 2001. MrBayes: bayesian inference of phylogenetic tree. Bioinformatics 17, 754–755.

Insel, N., Poulsen, C., Ehlers, T., 2009. Influence of the Andes Mountains on South American moisture transport, convection, and precipitation. Clim. Dynam. 35, 1477–1492.

Irestedt, M., Fjeldså, J., Ericson, P., Johansson, U.S., 2002. Systematic relationships and biogeography of the tracheophone suboscines (Aves: Passeriformes). Mol. Phylogenet. Evol. 23, 499–512.

Isler, M., Cuervo, A.M., Bravo, G.A., Brumfield, R.T., 2012. An integrative approach to species-level systematics reveals the depth of diversification in an Andean Thamnophilid, the Long-tailed Antbird. Condor 114, 571–583.

Kirby, M.X., Jones, D.S., MacFadden, B.J., 2008. Lower Miocene stratigraphy along the Panama Canal and its bearing on the Central American Peninsula. PLoS ONE 3, e2791.

Latrubesse, E.M., Cozzuol, M., Silva-Caminha, S.A.F., Rigsby, C.A., Absy, M.A., Jaramillo, C., 2010. The late Miocene paleogeography of the Amazon Basin and the evolution of the Amazon River system. Earth-Sci. Rev. 99, 99–124.

Lohmann, L.G., Bell, C.D., Calió, M.F., Winkworth, R.C., 2013. Pattern and timing of biogeographical history in the Neotropical tribe Bignonieae (Bignoniaceae). Bot. J. Linn. Soc. 171, 154–170.

Maldonado-Coelho, M., Blake, J.G., Silveira, L.F., Batalha-Filho, H., Ricklefs, R.E., 2013. Rivers, refuges and population divergence of fire-eye antbirds (*Pyriglena*) in the Amazon Basin. J. Evolution. Biol. 26, 1090–1107.

Matzke, N.J., 2013. Probabilistic historical biogeography: new models for founder-event speciation, imperfect detection, and fossils allow improved accuracy and model-testing. Frontiers Biogeography 5, 242–248.

Miller, M.A., Pfeiffer, W., Schwartz, T., 2010. Creating the CIPRES science gateway for inference of large phylogenetic trees. In: Proceedings of the Gateway Computing Environments Workshop (GCE), 14 November 2010, New Orleans, pp. 1–8.

Moyle, R.G., Chesser, R.T., Brumfield, R.T., Tello, J.G., Marchese, D.J., Cracraft, J., 2009. Phylogeny and phylogenetic classification of the antbirds, ovenbirds, woodcreepers, and allies (Aves: Passeriformes: infraorder Furnariides. Cladistics 25, 386–405.

Moritz, C., Patton, J.L., Schneider, C.J., Smith, T.B., 2000. Diversification of rainforest faunas: an integrated molecular approach. Annu. Rev. Ecol. Syst. 31, 533–563.

Myers, N., Mittermeier, R.A., Mittermeier, C.G., da Fonseca, G.A.B., Kent, J., 2000. Biodiversity hotspots for conservation priorities. Nature 403, 853–858.

Nee, S., Mooers, A.O., Harvey, P.H., 1992. Tempo and mode of evolution revealed from molecular phylogenies. Proc. Natl. Acad. Sci. USA 89, 8322–8326.

Nylander, J.A.A., 2004. MrModeltest 2.2. Program Distributed by the Author. Evolutionary Biology Centre, Uppsala University.

Ohlson, J.I., Irestedt, I., Ericson, P.G.P., Fjeldså, J., 2013. Phylogeny and classification of the New World suboscines (Aves, Passeriformes). Zootaxa 3613, 1–35.

Paradis, E., Claude, J., Strimmer, K., 2004. APE: analyses of phylogenetics and evolution in R language. Bioinformatics 20, 289–290.

Patel, S., Weckstein, J.D., Patané, J.S.L., Bates, J.M., Aleixo, A., 2011. Temporal and spatial diversification of *Pteroglossus* araçaris (Aves: Ramphastidae) in the neotropics: constant rate of diversification does not support an increase in radiation during the Pleistocene. Mol. Phylogenet. Evol. 58, 105–115.

Pybus, O.G., Harvey, P.H., 2000. Testing macro-evolutionary models using incomplete molecular phylogenies. Proc. R. Soc. B 267, 2267–2272.

R Development Core Team, 2012. R: a language and environment for statistical computing. R Foundation for Statistical Computing, Vienna, Austria. <http://www.R-project.org>.

Rabosky, D.L., 2006. Likelihood methods for detecting temporal shifts in diversification rates. Evolution 60, 1152–1164.

Ree, R.H., Moore, B.R., Webb, C.O., Donoghue, M.J., 2005. A likelihood framework for inferring the evolution of geographic range on phylogenetic trees. Evolution 59, 2299–2311.

Ree, R.H., Smith, S.A., 2008. Maximum likelihood inference of geographic range evolution by dispersal, local extinction, and cladogenesis. Syst. Biol. 57, 4–14.

Remsen, J.V., Jr., Cadena, C.D., Jaramillo, A., Nores, M., Pacheco, J.F., Pérez-Emán, J., Robbins, M.B., Stiles, F.G., Stotz, D.F., Zimmer, K.J., 2013. A classification of the bird species of South America (version: 20 May 2013). American Ornithologists' Union. <http://www.museum.lsu.edu/~Remsen/SACCBaseline.html>.

Ribas, C.C., Moyle, R.G., Miyaki, C.Y., Cracraft, J., 2007. The assembly of montane biotas: linking Andean tectonics and climatic oscillations to independent regimes of diversification in *Pionus* parrots. Proc. R. Soc. B 274, 2399–2408.

Ribas, C.C., Miyaki, C.Y., Cracraft, J., 2009. Phylogenetic relationships, diversification, and biogeography in Neotropical *Brotogeris* parakeets. J. Biogeogr. 36, 1712–1729.

Ribas, C.C., Aleixo, A., Nogueira, A.C.R., Miyaki, C.Y., Cracraft, J., 2012. A palaeobiogeographic model for biotic diversification within Amazonia over the past three million years. Proc. R. Soc. B 279, 681–689.

Rice, N.H., 2005. Phylogenetic relationships of antpitta genera (Passeriformes: Formicariidae). Auk 122, 673–683.

Ricklefs, R.E., 2002. Splendid isolation: historical ecology of the South American passerine fauna. J. Avian Biol. 33, 207–211.

Ridgely, R., Tudor, G., 1994. The Birds of South America, The Suboscine Passerines, vol. II. University of Texas Press, Austin.

Ridgely, R.S., Allnutt, T.F., Brooks, T., McNicol, D.K., Mehlman, D.W., Young, B.E., Zook, J.R., 2003. Digital Distribution Maps of the Birds of the Western Hemisphere, version 1.0. NatureServe, Arlington, VA.

Rull, V., 2008. Speciation timing and Neotropical biodiversity: the Tertiary-Quaternary debate in the light of molecular phylogenetic evidence. Mol. Ecol. 17, 2722–2729.

Rull, V., 2011a. Neotropical biodiversity: timing and potential drivers. Trends Ecol. Evol. 26, 508–513.

Rull, V., 2011b. Origins of biodiversity. Science 331, 398–399.

Rull, V., 2013. Palaeoclimates and Amazon biodiversity. J. Biogeogr. 40, 1413–1414.

Sambrook, J., Fritschi, E.F., Maniatis, T., 1989. Molecular cloning: a laboratory manual. Cold Spring Harbor Laboratory Press, New York.

Schulenberg, T.S., Stotz, D.S., Lane, D.F., O'Neill, J.P., Parker III, T.A., 2010. Birds of Peru: Revised and Updated Edition. Princeton University Press, New Jersey.

Silva, J.M.C., 1995. Biogeographic analysis of the South American Cerrado avifauna. Steenstrupia 21, 49–67.

Smith, B.T., Klicka, J., 2010. The profound influence of the late Pliocene Panamanian uplift on the exchange, diversification, and distribution of New World birds. Ecography 33, 333–342.

Stamatakis, A., Hoover, P., Rougemont, J., 2008. A fast bootstrapping algorithm for the RAxML web-servers. Syst. Biol. 57, 758–771.

Swofford, D.L., 1998. Paup∗. Phylogenetic analysis using parsimony (∗ and other methods), v. 4, Sunderland, MA, Sinauer.

Tamura, K., Peterson, D., Peterson, N., Stecher, G., Nei, M., Kumar, S., 2011. MEGA5: molecular evolutionary genetics analysis using maximum likelihood, evolutionary distance, and maximum parsimony methods. Mol. Biol. Evol. 28, 2731–2739.

Upham, N.S., Ojala-Barbour, R., Brito, J., Velazco, P.M., Patterson, B.D., 2013. Transitions between Andean and Amazonian centers of endemism in the radiation of some arboreal rodents. BMC Evol. Biol. 13, 191.

Vanzolini, P.E., Williams, E.E., 1970. South American anoles: the geographic differentiation and evolution of the *Anolis chrysolepis* species group (Sauria: Iguanidae). Arquiv. Zool. (S. Paulo) 19, 1–298.

Wallace, A.R., 1852. On the monkeys of the Amazon. Proc. Zool. Soc. London 20, 107–110.

Weir, J.T., Bermingham, E., Schluter, D., 2009. The Great American biotic interchange in birds. Proc. Natl. Acad. Sci. USA 106, 21737–21742.

Weir, J.T., Schluter, D., 2008. Calibrating the avian molecular clock. Mol. Ecol. 17, 2321–2328.

Weir, J.T., Price, M., 2011. Andean uplift promotes lowland speciation through vicariance and dispersal in *Dendrocincla* woodcreepers. Mol. Ecol. 20, 4550–4563.

Wesselingh, F.P., Räsänen, M.E., Irion, G., Vonhof, H.B., Kaandorp, R., Renema, W., Romero Pittman, L., Gingras, M., 2002. Lake Pebas: a palaeoecological reconstruction of a Miocene, long-lived lake complex in western Amazonia. Cainozoic Res. 1, 35–81.

Whitney, B.M., 2003. Family Conopophagidae (Gnateaters). In: del Hoyo, J., Elliot, A., Christie, D.A., (Eds.), Handbook of the birds of the world, Vol. 8. Lynx Edicions, Barcelona, pp. 732–748.

Whitmore, T.C., Prance, G.T., 1987. Biogeography and Quaternary History in Tropical America. Oxford University Press, New York.

Wilkinson, M.J., Marshall, L.G., Lundberg, J.G., Kreslavsky, M.H., 2010. Megafan environments in northern South America and their impact on amazon neogene aquatic ecosystems. In: Hoorn, C., Wesselingh, F. (Eds.), Amazonia, Landscape and Species Evolution: A Look into the Past. Wiley-Blackwell, Oxford, pp. 162–184.

Willis, E.O., 1992. Zoogeographical origins of eastern Brazilian birds. Ornit. Netrop. 3, 1–15.